Atmospheric Environment Vol. 15, No. 10/11, pp. 2171–2177, 1981
Printed in Great Britain.

0004-6981/81/102171-07 $02.00/0

THE EFFECTS OF NO_2–AEROSOL INTERACTION ON INDICES OF PERCEIVED VISIBILITY IMPAIRMENT*

PETER J. HAAS and ALLAN J. FABRICK

Radian Corporation, Austin, Texas, U.S.A.

(*First received* 2 *September* 1980 *and in final form* 26 *January* 1981)

Abstract—This paper discusses the effects of NO_2 and sulfate aerosols on visibility indices predicted by a plume visibility model. Calculations are performed over a range of ambient conditions and pollutant concentrations consistent with large power plants located in rural western U.S.A. Analysis of model equations and numerical results showed that NO_2 and sulfate concentrations effect visibility impairment indices in a complex manner. Because the NO_2–sulfate interactions are highly dependent on ambient conditions, designers of screening analysis procedures should consider such effects. The methodology used in this study is applicable to model validation efforts.

INTRODUCTION

The quantification and prediction of visibility impairment by point source plumes has become an important legislative concern. Sections 165(d) and 165(e) of the Clean Air Act require that a visibility analysis be performed for all proposed major emitting facilities. The U.S. Environmental Protection Agency is currently formulating procedures for performing these visibility analyses.

A significant assumption underlying the proposed visibility analysis procedures is that visibility impairment can be divided into two distinct classes: contrast reduction caused by sulfate aerosol haze and atmospheric discoloration caused by nitrogen dioxide (NO_2). The purpose of this paper is to explore the effects of NO_2–sulfate aerosol interactions upon predicted values of five indices of perceived visibility impairment. A modified version of the plume visibility model developed for the EPA (Latimer *et al.*, 1980) was used to relate ambient variables (pollutant concentrations, solar angle, observer–plume configuration, ambient visibility, humidity, etc.) to the visibility impairment indices. The model was run for over 4000 combinations of NO_2 and SO_4 concentrations, plume-observer-target distances, solar scattering angles, and ambient visibilities. The results of the model simulations were combined with an analysis of the model equations to characterize the effects of NO_2–SO_4 interactions upon predicted visibility impairment.

It should be noted that the EPA model has not yet been fully validated, so that the results presented here represent model predictions and not necessarily real world phenomena. However, since the EPA has proposed this model as a required tool for visibility analysis, this paper has several purposes: (1) to extend the range of visibility impairment parameters predicted by the model; (2) to direct future model validation efforts by providing insights into the behavior of the impairment indices as predicted by the EPA model; (3) to indicate a methodology for using the EPA model in a conservative fashion; (4) to indicate a methodology for analyzing the behavior of other visibility models and (5) to evaluate the performance of the visibility impairment indices, and to analyze several model-independent inconsistencies between them.

INDICES OF VISIBILITY IMPAIRMENT

Visible radiation is attenuated by both scattering and absorption as it propagates through the atmosphere. A plume further alters the light passing through it. In a power plant using state of the art control technology, primary particulate emissions are so low that the primary attenuation processes are scattering by secondary sulfate particles and absorption by NO_2 molecules.

If fly ash emissions are significant, scattering and absorption by primary particulates would have to be considered in addition to sulfate and NO_2 effects. For the present analysis, particulate emissions are assumed to be stringently controlled.

Attenuation processes are wavelength dependent. It is well known, for example, that NO_2 will selectively absorb blue light, producing a brownish discoloration of the sky.

Figure 1 is a schematic representation of vision

* Paper presented at the Symposium on Plumes and Visibility: Measurements and Model Components. Grand Canyon, Arizona, U.S.A. 10–14 November 1980.

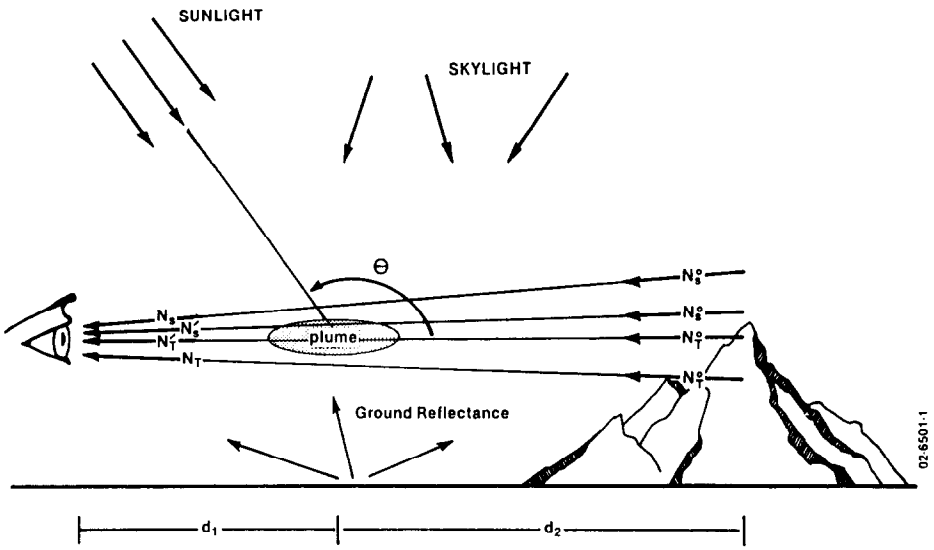

Fig. 1. Schematic representation of vision through the atmosphere.

through the atmosphere. N_S° and N_T° are the inherent sky and target radiances, N_S and N_T are the observed radiances in the absence of a plume, and N'_S and N'_T are sky and target radiances as viewed through the plume. Visibility impairment is clearly related to the way in which these radiance values are perceived. Human visual perception is believed to be dependent upon relative light intensity and wavelength differences, so that simultaneous measures of contrast at multiple wavelengths can completely characterize visibility impairment (Malm *et al.*, 1980). By comparing different radiance values at different wavelengths, various indices of visibility impairment are obtained.

Indices which simultaneously measure radiance differences at several wavelengths are usually referred to as color contrast or discoloration indices. Contrast indices, simpler measures of visibility impairment, only measure radiance differences at a single wavelength.

A measure of the reduction in perceived sky–target contrast caused by a plume, ΔC, may be defined as:

$$\Delta C = \left|\frac{N_t}{N_s} - 1\right| - \left|\frac{N'_t}{N'_s} - 1\right|. \tag{1}$$

The radiance values are evaluated at a wavelength of 550 nm, corresponding to the wavelength of peak human visual response.

Another indicator of plume visibility is the contrast of a plume against the sky, C_p. In terms of radiance values,

$$C_p = \frac{N'_s}{N_s} - 1. \tag{2}$$

Again, the calculation is performed at 550 nm. If C_p is greater or less than 1, the plume will appear brighter or darker, respectively, than the background sky.

The blue/red luminance ratio, B/R, is a measure of the discoloration of the background sky by the plume. Letting $C_p(\lambda)$ denote plume/sky contrast evaluated at wavelength λ, B/R is defined (Latimer and Samuelson, 1975) as follows:

$$B/R = \frac{C_p(400)+1}{C_p(700)+1}. \tag{3}$$

A value of B/R greater or less than 1 corresponds to a plume looking respectively "bluer" or "browner" than the adjacent background sky.

Analogs to ΔC and C_p that consider changes not only in brightness, but also in color, are the color contrast parameters CC and ΔCC proposed by Malm *et al.* (1980). In this formalism, radiance values, N, are converted into red, green and blue luminance values, L_r, L_g and L_b by combining the radiance values with the red, green and blue spectral response curves of the human eye. Using L values instead of radiances, red, blue, and green analogs of C_p and ΔC can be calculated: C_p^r, C_p^b, C_p^g where:

$$C_p^i = 1 - F\left[\frac{L_i^c}{\max(L_i^c, L_i^p)}\right]. \tag{4}$$

C_p^i is the plume/sky contrast for the i-th color and L_i^p and L_i^c are sky luminance values for color i with and without the plume, respectively. The quality in brackets is the luminance of the plume (at color i) relative to the lightest luminance (at color i) in the field view. The function $F[\cdot]$ maps relative luminances into uniformly perceived "brightness values". The function was derived from psychophysical experiments conducted by Land (1977).

The color contrast vector **CC** can be defined as

$$\mathbf{CC} = |C_p^r|\hat{i} + |C_p^g|\hat{j} + |C_p^b|\hat{k}. \tag{5}$$

CC will uniquely specify plume color in a three-dimensional color space. An illustration of this color space may be found in Land (1977).

An average color contrast for a vista can be defined (Malm *et al.*, 1980) by

$$CC = \int_{\text{All Area}} P(\text{area})|\bar{C}'(\text{area})|d(\text{area}). \quad (6)$$

CC is the average vista color contrast while P(area) is the fraction of the total scene that has a given color contrast $\bar{C}'$. $|\bar{C}'(\text{area})|$ is, then, the magnitude of color contrast of a specific area and d(area) is the incremental area associated with each unique color.

For the present analysis a simplified vista consisting of uniform sky and terrain was used for ΔCC calculations. With this simplifying assumption, the integral in Equation (6) may be replaced by a weighted average of sky and terrain color contrast magnitudes. The reduction in average vista color contrast, ΔCC, is then defined by

$$\Delta CC = CC - CC' \quad (7)$$

where CC' and CC are the average color contrast values for a sky/terrain vista with and without the plume, respectively. Centerline plume concentrations were used in this study to calculate ΔCC at all points in the vista, a presumably conservative approach.

Other indices of visibility impairment are reduction in visual range, ΔVR, and ΔE, the change in luminance and chromaticity coordinates referred to as the color change parameter by Latimer *et al.* (1978). Because of theoretical problems associated with these indices (Malm, 1979; Malm *et al.* 1980; Henry, 1979) neither were considered in this analysis.

MODELING PROCEDURE

A complete description of the plume visibility model may be found in Latimer *et al.* (1978). The full visibility model uses dispersion and chemical kinetics submodels to predict ambient, crosswind-integrated pollutant concentrations. An atmospheric optics submodel is then used to relate pollutant concentrations to radiance values at the observer's location. The radiance values are then used to compute visibility impairment indices. For the current study, a range of representative concentration values were selected and input directly into the atmospheric optics submodel, bypassing the dispersion and chemical transformation calculations. The optics model was streamlined, and modified to calculate the CC, ΔC and ΔCC indices.

The atmospheric optics submodel is based upon an analytical solution to an approximate form of the equation of radiative transfer. The most important simplifying assumptions in the model are: (i) plane-parallel background atmosphere consisting of two homogeneous layers; (ii) average solar flux and diffuse intensity ground reflectance of 0.3; (iii) negligible effect of the plume on solar flux (optically thin plume); (iv) spherical particles and (v) lognormal aerosol size distributions.

In addition to these model assumptions, the following was also assumed: (i) 10% relative humidity; (ii) target reflectance of 0.3; (iii) particle size distribution parameters given in Table 1; (iv) no ambient NO_2 or coarse mode aerosol; (v) calculations performed at sea level and (vi) terrain occupies 1/3 of vista.

If we additionally assume that the observer looks horizontally across the plume towards a vista in the distance, and that the sun, plume and observer are oriented such that the sight path lies parallel to the solar azimuth and perpendicular to the plume centerline, then calculations of visual impairment indices can be made given six independent variables. These variables are: the centerline crosswind integrated NO_2 concentration ($\overline{NO}_2$); the centerline crosswind integrated sulfate aerosol concentration ($\overline{SO}_4$); the ambient visual range (VR); the distance between the observer and the plume centerline (d_1) the distance between the plume centerline and the vista (d_2) and the solar scattering angle (θ). These variables are illustrated in Fig. 1.

Table 1. Particle size distributions*

Aerosol type	Mass median radius (μm)	Geometric standard deviation (μm)	Particle density (g cm^{-3})
Background accumulation mode	0.35	2.10	1.50
Background coarse mode	6.00	2.20	2.50
Plume secondary sulfate	0.35	2.10	1.50

* There is considerable uncertainty in the size distributions of both natural and anthropogenic aerosols. To limit the current analysis to a tractable number of independent variables, the size distributions were held fixed. It is anticipated, for example, that decreasing the mass median radius for plume secondary sulfate would not change the qualitative results of the study, but would reduce the ambient sulfate concentrations required to produce a given visual effect. This should, of course, be verified.

Centerline cross wind integrated concentrations of NO_2 and SO_4 were calculated using a standard Gaussian plume model modified to incorporate first order sulfate chemistry and ozone-limited NO → NO_2 conversion (Haas, 1980). Pollutant emissions are representative of a new 2000 MW coal-fired power facility burning western coal and using best available control technology (Wolfe *et al.*, 1980). The results of these calculations are summarized in Fig. 2.

The range of values for the visibility model input parameters are summarized in Table 2. The visual range and observer plume-vista distances were selected as representative of values expected for the analysis of visibility impairment in the western U.S.A. The solar scattering angles represent forward scattering, sun directly overhead and backward scattering situations. Although the number of data points describing the range of values for each parameter is small, this input set represents 4320 visibility calculations. The predicted visual impairment indices were stored as a multidimensional array to facilitate analysis and interpretation of this large amount of data.

Table 2. Visibility model input parameters

Parameter	Value	Units
$\overline{NO_2}$	0, 200, 350, 500	mg m^{-2}
$\overline{SO_4}$	0, 1, 35, 75	mg m^{-2}
VR	100, 200, 300	km
d_1	1, 5, 10, 20, 40, 80	km
d_2	10, 20, 40, 80, 160	km
θ	45, 90, 135	degrees

RESULTS

The results of the theoretical and numerical analysis are given below for each of the five visual impairment parameters evaluated.

1. ΔC: From the fundamental model equations (Latimer *et al.*, 1978) it may be shown that

$$\Delta C = C\left(\frac{E}{k+E}\right) \tag{8}$$

where C is the perceived sky-target contrast in the absence of the plume, k is a positive constant independent of plume properties and E is a non-negative monotonically increasing function of both $\overline{SO_4}$ and $\overline{NO_2}$. It follows that ΔC is also a non-negative, monotonically increasing function of $\overline{SO_4}$ and $\overline{NO_2}$. The numerical results verify this conclusion. Whether ΔC obeyed the principle of superposition, i.e.,

$$\Delta C(\overline{SO_4}, O) + \Delta C(O, \overline{NO_2}) = \Delta C(\overline{SO_4}, \overline{NO_2}) \tag{9}$$

was also investigated. Using Equation (8) it can be shown that Equation (9) is equivalent to

$$k^2(E_n + E_s) + 2kE_nE_s + E_nE_sE_{ns} = k^2E_{ns} \tag{10}$$

where $E_s = E(\overline{SO_4}, O)$; $E_n = E(O, \overline{NO_2})$; $E_{ns} = E(\overline{SO_4}, \overline{NO_2})$. It can also be shown that the right hand side (RHS) of Equation (10), [and hence the RHS of Equation (9)], can be less than, equal to, or greater than the left hand side (LHS). This implies that $\overline{SO_4}$, when combined with $\overline{NO_2}$, can produce synergistic effects. However, model simulations indicated that the LHS of Equation (9) was within 1–3% of the RHS over the

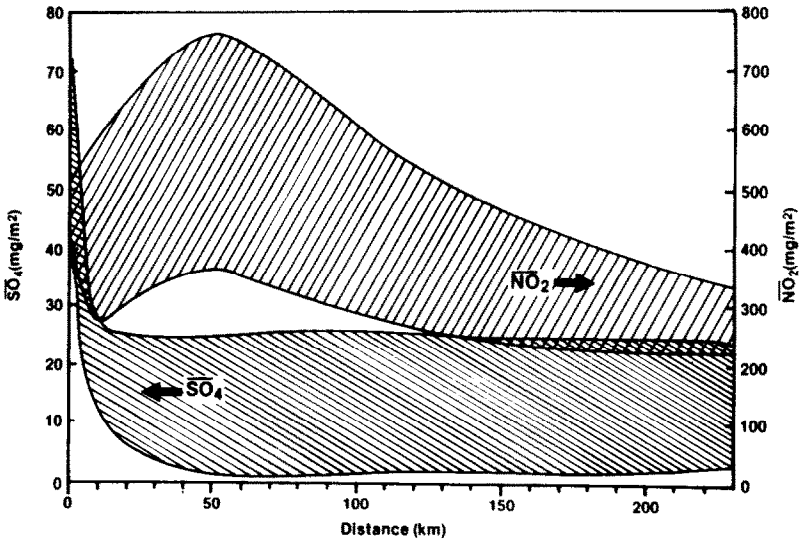

Fig. 2. Centerline crosswind integrated sulfate and nitrogen dioxide concentrations from a new 2000 MW Western Coalfired Power Generation Facility* as a function of downwind distance: Emissions: SO_2 407 g s^{-1}, SO_4 21 g s^{-1}, NO 1289 g s^{-1}, NO_2 143 g s^{-1}. Background ozone—40–80 ppb. Atmospheric stability—D and E. Wind Speed—5 m s^{-1}. SO_2 → SO_4 .05% – 2%/h. NO → NO_2 ozone limited method.

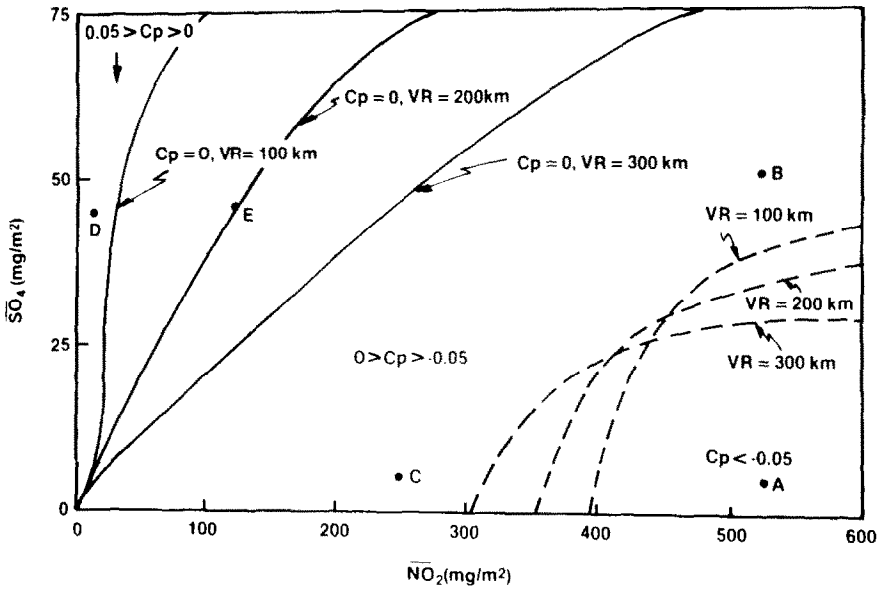

Fig. 3. Behavior of plume contrast, C_p, as a function of inegrated NO_2 and sulfate concentration and visual range: solar scattering angle, $\theta = 45°$; observer-plume distance, $d_1 = 5$ km; plume-target distance, $d_2 = 40$ km.

range of input values evaluated. (The LHS was larger at low visual ranges while the RHS was larger at high visual ranges, the interactions being more pronounced at high visual ranges.) Under a wide range of conditions, the assumption of superposition appears valid. Other results reflect some well-known properties of ΔC: ΔC is strongly dependent upon ambient visual range and $\overline{SO_4}$. ΔC is also very sensitive to plume-observer distance, with particularly complex effects occurring for NO_2-dominated plumes. Contrast reduction effects are most pronounced for forward-scattering ($\theta = 45°$).

2. C_p: Using the model equations, C_p can be written in the form

$$C_p = \left[k_1 \left(\frac{k_2 \overline{SO_4}}{k_2 \overline{SO_4} + k_3 \overline{NO_3}} \right) - k_4 \right] \times [1 - \exp(-k_2 \overline{SO_4} - k_3 \overline{NO_3})].$$

By holding all other variables fixed and varying the relative amounts of $\overline{NO_2}$ and $\overline{SO_4}$, C_p can be made greater than, less than, or equal to zero. When other variables are also varied, the behavior of C_p becomes quite complex. The behavior of C_p as a function of $\overline{NO_2}$, $\overline{SO_4}$, and ambient visual range, VR is illustrated in Fig. 3. The solid lines represent lines of zero C_p at several values of VR. Assuming a perceivable contrast threshold of $|C_p| = 0.05$, the dashed lines represent the minimum detectable value of C_p (for a dark plume) for several values of VR. For a given value of VR, a point lying below the corresponding dashed line will be visible as a dark plume. A point lying above the dashed line will be invisible. The dashed lines for a white plume do not lie on the graph. Hence, none of the $\overline{SO_4}/\overline{NO_2}$ combinations in Fig. 3 will yield a visible white plume (though a pure SO_4 plume will always be slightly brighter than the background sky). It can be seen that adding SO_4 to a visible dark plume (i.e., moving vertically from point A to point B) will mask the NO_2 absorption and render the plume undetectable according to the C_p index.* The better the ambient visibility, the more effective the sulfate scattering (see above discussion on ΔC), and the less SO_4 is needed to render the plume invisible. Similarly, adding NO_2 to an invisible dark plume (i.e., moving horizontally from point C to point A) will render the plume visible by darkening it further. The better the ambient visibility the less $\overline{NO_2}$ is needed to render the plume visible. It can also be seen that adding NO_2 to a slightly white plume (i.e. from point D to point E) will bring C_p to zero. The poorer the ambient visibility, the less $\overline{NO_2}$ will be needed. These results were obtained for the case of forward scattering. For the cases of 90° and backward scattering, $|C_p|$ is a monotonically increasing function of $\overline{NO_2}$ and $\overline{SO_4}$, hence, there is no masking effect, and adding SO_4 to a dark plume will only make the plume darker. In general, as θ increased so did $|C_p|$. These results agree with the well known fact that by changing the solar zenith angle (and hence the scattering angle) a given plume will appear dark, light or invisible, according to the C_p index.

3. B/R: The numerical simulation illustrated the strong dependence of B/R on $\overline{NO_2}$. B/R is only weakly dependent upon VR. As ambient visibility improves,

* It should be noted that for several values of NO_2 and SO_4, the C_p index indicated that the plume should be invisible, but the B/R index indicated a visible plume.

plume discoloration of the sky, as indicated by B/R, becomes more noticeable. For a plume without any $\overline{NO_2}$, the plume was slightly bluish-grey for forward scattering and slightly brown for back scattering, but these discoloration effects are probably not perceptible. As illustrated in Fig. 4, adding SO_4 to an NO_2 plume may reduce the NO_2 discoloration effect by scattering additional blue light toward the observer, reducing plume visual impacts in a manner similar to C_p. This effect, which has been noted by Latimer (1980), appears to be more significant under conditions of low ambient visibility.

4. CC: Several qualitative effects were observed during the numerical simulation. As $\overline{NO_2}$ increases, the plume always appears more brown. On the other hand, adding $\overline{SO_4}$ to an $\overline{NO_2}$ plume reduces the predicted discoloration for the case of forward scattering in a manner similar to C_p. For the case of backward scattering, adding SO_4 or $\overline{NO_2}$ to a plume will always cause the plume to appear more brown. This behavior is also similar to C_p. For the case of forward scattering, a pure SO_4 plume always appears white according to the CC index, even though the B/R index indicated a slightly discolored plume in some cases. As visual range or scattering angle increases, the plume, in general, appears more brown. However, for a pure NO_2 plume, the worst impacts are predicted to occur when the sun is overhead ($\theta = 90°$).

5. ΔCC: Since it was shown previously that ΔC was a positive monotonic increasing function of $\overline{SO_4}$ and $\overline{NO_2}$, it seems reasonable to expect that ΔCC would also be a monotonically increasing positive function. The numerical results support this assumption over the range of variables studied. The combined effects of NO_2 and SO_4 were always slightly greater than the sum of the individual effects, but the numerical results support the linearity assumption to within 4 per cent. It should also be noted that ΔCC is more sensitive to changes in $\overline{SO_4}$ than to changes in $\overline{NO_2}$.

CONCLUSIONS

The calculation of visibility impairment indices for a large range of ambient conditions demonstrates that when using the EPA model the effects of sulfate aerosols and NO_2 gas should be considered simultaneously to realistically quantify visibility impairments. NO_2 and sulfate aerosols, in general, affect the impairment indices in a non-linear fashion. NO_2–sulfate interactions may either diminish or enhance visibility impairment as calculated by considering each pollutant separately, depending upon ambient conditions. Care must therefore be taken when specifying worst-case conditions for simplified screening procedures. For example, screening analyses for plume contrast should be performed assuming backscattered solar radiation and should consider NO_2 and sulfate aerosols simultaneously. Similar cautions apply to other indices of visual impairment.

In general, the qualitative behavior of the color contrast indices is similar to that of their monochromatic counterparts. However, several inconsistencies between visual impairment indices have been identified

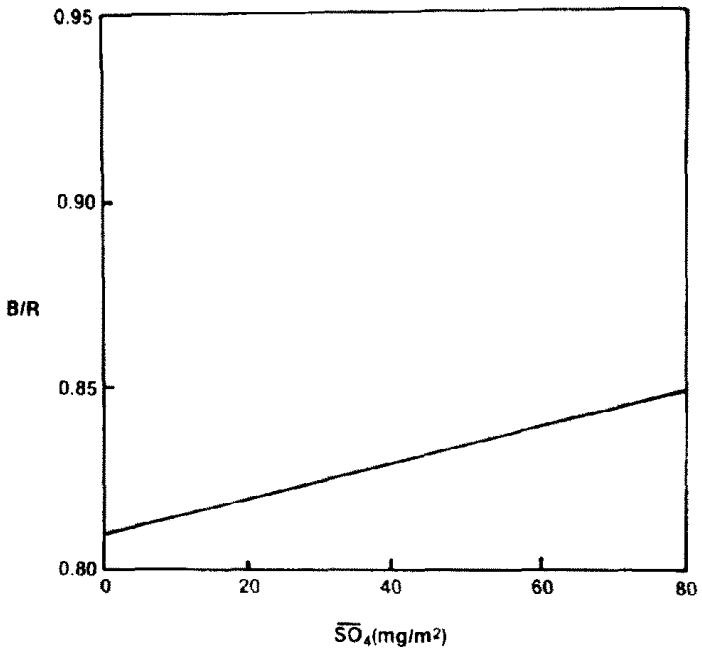

Fig. 4. Behavior of blue/red luminance ratio, B/R, as a function of integrated SO_4: solar scattering angle, $\theta = 45°$, observer-plume distance, $d_1 = 5$ km, plume-target distance, $d_2 = 40$ km, $\overline{NO_2} = 350$ mg m^{-2}, visual range = 100 km.

during this study. These inconsistencies are independent of the atmospheric optics model, since the impairment indices are computed from a common set of predicted radiance values. Plumes which are invisible according to one index (e.g. C_p) are visible according to another (e.g. B/R). There are also qualitative differences between the **CC** and B/R descriptions of pure sulfate plumes. Finally, the B/R, C_p and **CC** indices predict non-linear "masking" effects while the ΔC and ΔCC indices do not. One possible reason for the inconsistency between the B/R and C_p indices is that the C_p index only measures monochromatic radiance differences whereas the B/R index effectively compares C_p at two different points in the spectrum. Another possible reason for the discrepancy between the two indices may be the uncertainty surrounding the perception threshold values used for each index. More research is needed in order to identify consistent threshold values. The difference between the **CC** and B/R plume descriptions is probably due to the fact that the **CC** index takes into account the total eye–brain response to visual stimulae, while the B/R index ignores these psychophysical phenomena. The discrepancies between the "vista contrast" indices ΔC and ΔCC and the "plume contrast" indices B/R, C_p and **CC** may be attributed to the fact that two sets of indices are describing two different types of visual phenomena. By considering a terrain/sky vista as a visual "signal" transmitted toward the observer, the ΔC and ΔCC parameters may be interpreted as measures of a plume's tendency to reduce the "signal-to-noise ratio" in the perceived vista. On the other hand, the B/R, C_p and **CC** parameters measure not the obscuration of a visual target but the degree to which the spectral characteristics of the background sky are modified by the plume. According to the EPA model, these two visual phenomena are not equivalent. This hypothesis needs to be tested in the field. Clearly, more research is needed in order to further develop, evaluate and interpret appropriate indices of visibility impairment.

The relatively comprehensive description of the behavior of visibility impairment indices under a wide variety of ambient conditions developed for this study may be used as a standard of comparison in testing the visibility model against field data. The methodology described in this paper may also be used to examine the behavior and facilitate the validation of other visibility models.

For more extensive analyses, other parameters that should be varied include aerosol size distributions, ground albedo, particulate concentrations, and target sizes and reflectances.

REFERENCES

Environmental Protection Agency (1979) Protecting visibility: an EPA report to congress. EPA-405/5-79-008, Office of Air Quality Planning and Standards, Research Triangle Park, North Carolina, 311 pp.

Haas P. J. (1980) Final report: the VISMOD visibility screening model. DCN 80-241-005-05-04, Radian Corporation, Austin, Texas, 38 pp.

Henry R. C. (1979) The human observer and visibility: modern psychophysics applied to visibility degradation. *Proceedings of the Air Pollution Control Association Specialty Conference: View on Visibility Regulatory and Scientific*, Denver, Colorado, pp. 27–35.

Land E. H. (1977) The retinex theory of color vision. *Scient. Am.* **237**, 6, 108–128.

Latimer D. A. (1980) Power plant impacts on visibility in the west: siting and emissions control implications. *J. Air Pollut. Control Ass.* **30**, 142–146.

Latimer D. A. and Samuelsen G. S. (1975) Visual impact of plumes from power plants. UCI-ARTR-75-3, UCI Air Quality Laboratory, Irvine, California.

Latimer D. A., Bergstrom R. W., Hayes S. R., Lin M. K., Seinfeld J. H., Whitten G. Z., Wojcik M. A. and Hillyer M. J. (1978) *The Development of Mathematical Models for the Prediction of Anthropogenic Visibility Impairment*, Vols 1–3. EPA-450/3-78-110 a, b, c. U.S. Environmental Protection Agency, Office of Planning and Evaluation, Washington, D.C.

Malm W. C. (1979) Considerations in the Measurement of Visibility. *J. Air. Pollut. Control Ass.* **29**, 1042–1052.

Malm W. C., Leiker K. K., and Molenar J. V. (1980) Human perception of visual air quality. *J. Air Pollut. Control Ass.* **30**, 122–131.

Wolfe D. E., Fabrick A. J. and Stuart J. D. (1980) Air quality and visibility impact studies for the Allen–Warner Valley Energy System. DCN 80-241-005-05-02, Radian Corporation, Austin, Texas.